

SCIENTIFIC REPORTS

OPEN

An extracellular [NiFe] hydrogenase mediating iron corrosion is encoded in a genetically unstable genomic island in *Methanococcus maripaludis*

Hirohito Tsurumaru, Naofumi Ito, Koji Mori, Satoshi Wakai, Taku Uchiyama, Takao Iino , Akira Hosoyama, Hanako Ataku, Keiko Nishijima, Miyako Mise, Ai Shimizu, Takeshi Harada, Hiroshi Horikawa, Natsuko Ichikawa, Tomohiro Sekigawa, Koji Jinno, Satoshi Tanikawa, Jun Yamazaki, Kazumi Sasaki, Syuji Yamazaki, Nobuyuki Fujita & Shigeaki Harayama

Certain methanogens deteriorate steel surfaces through a process called microbiologically influenced corrosion (MIC). However, the mechanisms of MIC, whereby methanogens oxidize zerovalent iron (Fe^0), are largely unknown. In this study, Fe^0 -corroding *Methanococcus maripaludis* strain OS7 and its derivative (strain OS7mut1) defective in Fe^0 -corroding activity were isolated. Genomic analysis of these strains demonstrated that the strain OS7mut1 contained a 12-kb chromosomal deletion. The deleted region, termed “MIC island”, encoded the genes for the large and small subunits of a [NiFe] hydrogenase, the *TatA/TatC* genes necessary for the secretion of the [NiFe] hydrogenase, and a gene for the hydrogenase maturation protease. Thus, the [NiFe] hydrogenase may be secreted outside the cytoplasmic membrane, where the [NiFe] hydrogenase can make direct contact with Fe^0 , and oxidize it, generating hydrogen gas: $\text{Fe}^0 + 2\text{H}^+ \rightarrow \text{Fe}^{2+} + \text{H}_2$. Comparative analysis of extracellular and intracellular proteomes of strain OS7 supported this hypothesis. The identification of the MIC genes enables the development of molecular tools to monitor epidemiology, and to perform surveillance and risk assessment of MIC-inducing *M. maripaludis*.

The oxidation of zerovalent iron (Fe^0) is accelerated by metabolic activities of certain microorganisms through a process called microbiologically influenced corrosion (MIC). Sulfate-reducing bacteria (SRB) are considered the main causal agents of MIC under anaerobic conditions through the formation of hydrogen sulfide, which is a very corrosive compound¹. MIC induced by chemical reactions with biogenic compounds such as hydrogen sulfide is referred to as “chemical microbiologically influenced corrosion” or CMIC².

The cathodic depolarization theory is another proposed mechanism of MIC, which has attracted both support and criticism. This theory assumes that the anaerobic oxidation of Fe^0 ($\text{Fe}^0 \rightleftharpoons \text{Fe}^{2+} + 2\text{e}^-$; anodic reaction) coupled with the reduction of H^+ ($2\text{H}^+ + 2\text{e}^- \rightleftharpoons \text{H}_2$; cathodic reaction) is limited by the diffusion of H_2 from the cathode, and that hydrogenotrophic microorganisms including SRB and methanogens accelerate the rate-limiting cathodic reaction by consuming H_2 built up around Fe^0 surfaces. However, the validity of this theory was questioned, as not all hydrogenotrophic SRB and methanogens promoted Fe^0 corrosion^{3,4}.

On the other hand, Zadvorny and colleagues⁵ found that hydrogenases from *Thiocapsa roseopersicina* and *Lamrobacter modestohalophilus* accelerated the corrosion of Fe^0 and other metals with simultaneous evolution of H_2 . Based on the results, they proposed that the direct withdrawal of electrons from Fe^0 by the hydrogenases accelerates Fe^0 corrosion. Recently, Fe^0 corrosion due to direct electron withdrawal has attracted much attention, and this mechanism is termed “electrical microbiologically influenced corrosion” or EMIC². The direct electron transfer from an Fe^0 electrode to cells of the Fe^0 -corroding SRB, *Desulfohalobium ferrireducens* IS4³, was experimentally demonstrated⁶. Further electrochemical and infrared spectroelectrochemical analyses indicated that the direct

NITE Biological Resource Center (NBRC), National Institute of Technology and Evaluation (NITE), Chiba, 292-0818, Japan. Correspondence and requests for materials should be addressed to S.H. (email: harayama@bio.chuo-u.ac.jp)

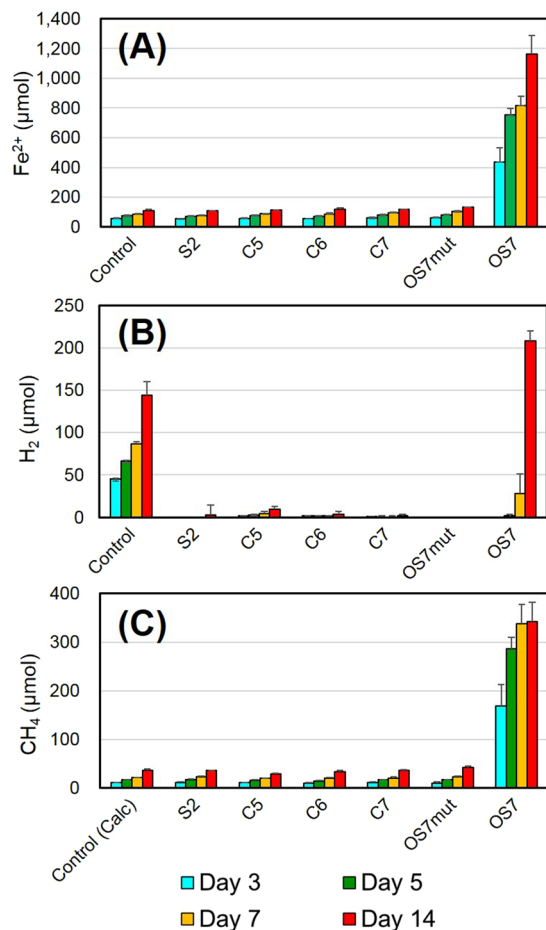


Figure 1. Fe⁰-corroding activities in various *M. maripaludis* strains. Amounts of Fe²⁺ in culture fluids (A), amounts of H₂ in headspace gas (B), and amounts of CH₄ in headspace gas (C) were determined after growth of the indicated strains for 3 to 14 days. Means and standard deviations of four determinations are shown. CH₄ was not detected in headspace gas of the control samples, but amounts of CH₄ which can be synthesized from H₂ generated in the control samples are shown as “Control (Calc)”.

electron transfer from Fe⁰ to cells of strain IS4 occurred via *c*-type cytochromes located on the cell surface⁷. *c*-type cytochromes have been found in the outer membranes of particular microorganisms, which have the ability to acquire energy through transfer of electrons to extracellular electron acceptors or from extracellular electron donors⁸. The direct electron transfer from Fe⁰ to the cells of another SRB, *Desulfovibrio ferrophilus* IS5³, was also demonstrated⁹.

Methanogenic archaea may be second only to SRB as the most common cause of MIC in anaerobic environments^{3,10–12}. Recently, Deutzmann *et al.*¹³ demonstrated that cell-free filtrates of spent cultures of the Fe⁰-corroding methanogen, *Methanococcus maripaludis* MM901, accelerated H₂ generation from Fe⁰, while filtrates of spent cultures of strain MM1284, which carried mutations in five hydrogenase genes and one dehydrogenase gene, did not accelerate it. Since the activity in the filtrate of strain MM901 was thermolabile and proteinase-sensitive, they concluded that enzyme(s), most probably hydrogenase(s) secreted from strain MM901, catalyzed the electron withdrawal from Fe⁰.

Previously, we isolated and characterized Fe⁰-corroding *M. maripaludis* KA1¹¹. In this study, we isolated another Fe⁰-corroding *M. maripaludis* strain, OS7, from which an Fe⁰-non-corroding mutant was isolated and characterized.

Results and Discussion

Isolation of Fe⁰-corroding *M. maripaludis* strain OS7 and its Fe⁰-non-corroding derivative, strain OS7mut1. An Fe⁰-corroding methanogen named strain OS7 was isolated from water sitting at the bottom of a crude-oil storage tank at Osaka by the method described previously for the isolation of Fe⁰-corroding *M. maripaludis* strain KA1¹¹. The 16S rRNA gene sequence of strain OS7 was 100% identical to the 16S rRNA gene sequence of the type strain of *M. maripaludis* (strain JJ^T); thus, strain OS7 was identified as belonging to the species *M. maripaludis*.

Similar to strain KA1, strain OS7 corroded Fe⁰ with concomitant CH₄ production (Fig. 1). The amount of Fe²⁺ dissolved in a culture of strain OS7 at day 7 (816 μmol from 20 ml culture) was almost 10-fold higher than that produced in a sterile control (86 μmol from 20 ml culture). On the other hand, *M. maripaludis* strains S2, C5, C6,

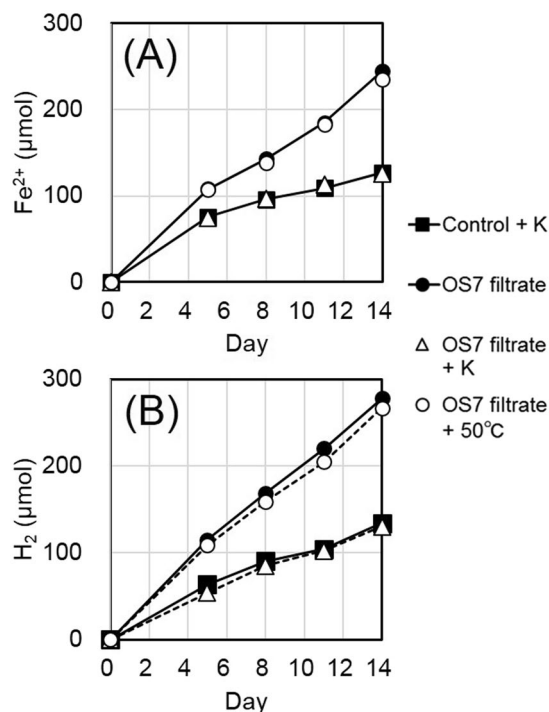


Figure 2. Fe⁰-corroding activities in filtrates of an OS7 culture. Filtrates of a culture of strain OS7 grown for 10 days under H₂ + CO₂ (80:20) were prepared, and 1 ml of the filtrate was added to 20 ml of basal medium containing Fe⁰ granules either without treatment (OS7 filtrate), or with proteinase K treatment at 50 °C for 20 min and at 100 °C for 5 min (OS7 filtrate + K), or with treatment at 50 °C for 20 min (OS7 filtrate + 50 °C). As a control, 21-ml basal medium containing Fe⁰ granules was treated with proteinase K at 50 °C for 20 min and at 100 °C for 5 min (Control + K). Duplicate samples of each treatment were incubated at 37 °C for 5, 8, 11 and 14 days, and the amounts of Fe²⁺ in basal medium (A), and amounts of H₂ in headspace gas (B) were determined. The amounts of CH₄ in headspace gas were also determined, and were zero in all samples.

and C7 acquired from culture collections did not show enhanced Fe⁰ corrosion (Fig. 1(A)). The small amount of CH₄ detected in the cultures of these strains (Fig. 1(B)) was interpreted to be synthesized by them using H₂ generated by spontaneous Fe⁰ oxidation [see Fig. 1(C) “Control (Calc)”].

Previously, rapid Fe⁰ corrosion concomitant with rapid H₂ evolution was observed with spent culture filtrates of *M. maripaludis* MM901¹³. In agreement with this, culture filtrates of strain OS7 also accelerated Fe⁰ dissolution and H₂ evolution when they were added in basal medium containing Fe⁰ granules under a N₂ + CO₂ atmosphere (Fig. 2, OS7 filtrate). However, the evolution of CH₄ was not detected in this instance. The culture filtrates treated with proteinase K at 50 °C for 20 min followed by heat-treatment at 100 °C for 5 min completely lacked the ability to enhance Fe⁰-dissolution and H₂ evolution (OS7 filtrate + K), while the treatment of culture filtrates at 50 °C for 20 min did not affect these activities (OS7 filtrate + 50 °C). These observations suggested that the enhanced Fe⁰-dissolution (MIC activity) and H₂ evolution were catalyzed by an enzyme such as a hydrogenase secreted from cells of strain OS7.

We noticed that strains OS7 and KA1 lost their MIC activity when they had been continuously grown under H₂ + CO₂. From one of such cultures of strain OS7, one clone named strain OS7mut1 was isolated by the agar shake tube technique^{14,15}. As shown in Fig. 1, strain OS7mut1 exhibited neither enhanced Fe⁰ dissolution nor enhanced CH₄ production in basal medium containing Fe⁰ granules. Furthermore, culture filtrates of strain OS7mut1 showed neither enhanced Fe⁰ dissolution nor enhanced H₂ evolution.

Whole genome sequencing of Fe⁰-corroding *M. maripaludis* strains. The whole genome sequences of strains OS7 and KA1 were determined. The genome of strain KA1 contained a circular 1,846,330 bp chromosome and a circular 12,084 bp plasmid, while that of strain OS7 contained a circular 1,749,749 bp chromosome but no plasmid. The G+C content of both OS7 and KA1 were 32.9 (mol)%.

We assumed that the genes involved in Fe⁰ corrosion exist in the genomes of Fe⁰-corroding strains OS7 and KA1, but are absent in the genomes of Fe⁰-non-corroding strains such as strains S2, C5, C6, and C7. We then identified genes unique to strains OS7 and KA1 by analyzing reciprocal best hits between the genomes of these strains. A total of 72 genes were identified to be specific to strains OS7 and KA1 (Table S1).

Proteomics analyses of culture filtrates of strains OS7 and OS7mut1. Although the reciprocal best-hit approach identified 72 candidate genes involved in Fe⁰ corrosion, it was necessary to further narrow this number down. We then performed proteomic analysis of culture filtrates of strains OS7 and OS7mut1, as MIC activity was detected in the culture filtrates of strain OS7 (Fig. 2), but not in those of strain OS7mut1. Proteins in

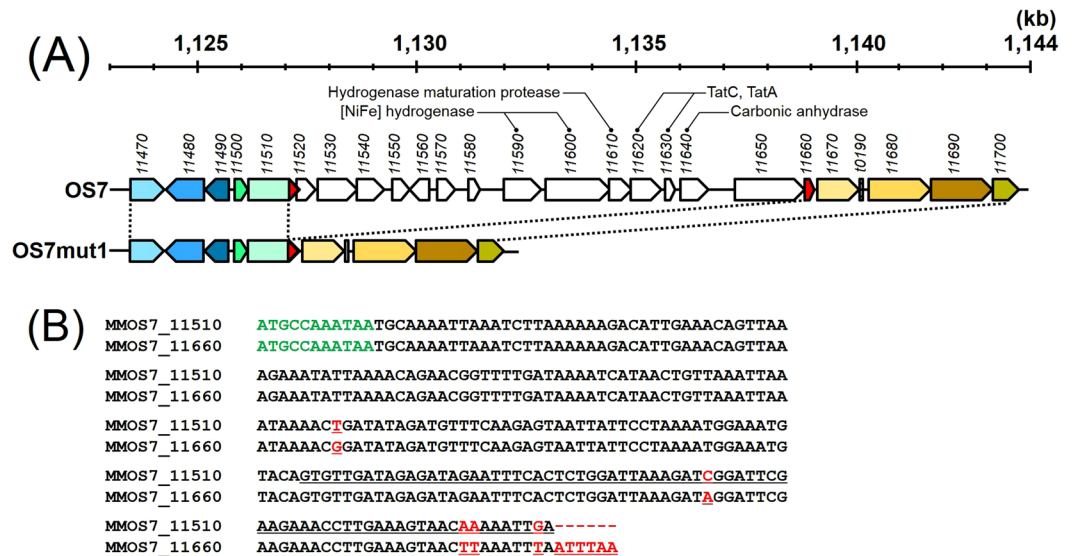


Figure 3. (A) Genome map of strain OS7 at coordinates 1,123 to 1,144 kb and that of strain OS7mut1 at the corresponding region. Numbers below the genome coordinates indicate locus tags (*MMOS7_number*). Homologous genes between the two genomes are shown in the same colors. The 3'-end sequence of *MMOS7_11510* and the 5'-end sequence of *MMOS7_11660* were almost identical; these sequences are shown in red. The gene cluster named “the MIC island” (*MMOS7_11520*–*MMOS7_11650*) is absent in the genome of strain OS7mut1. (B) Alignment of the nucleotide sequence of the 3'-end of *MMOS7_11510* and that of *MMOS7_11660*. The upper sequence shows the 3'-end sequence of *MMOS7_11510*, the last three bases (TGA) being a stop codon, while the lower sequence shows the *MMOS7_11660* sequence, the first three bases (ATG) and the last three bases (TAA) being the initiation and stop codons, respectively. Mismatched sequences are shown in red and underlined. The 3'-end region of the nucleotide sequence of the *MMOS7_11510*/*MMOS7_11660* hybrid gene in strain OS7mut1 was 100% identical to that of *MMOS7_11660*. The nucleotide sequence of the whole *MMOS7_11510*/*MMOS7_11660* hybrid gene in strain OS7mut1 was 100% identical to the sequences of the corresponding genes in *M. maripaludis* strains, S2, C5, C6, and C7.

culture filtrates of strains OS7 and OS7mut1 were subjected to trypsinolysis, and analyzed by nano-ESI–MS/MS followed by Mascot searches against the gene products of the OS7 genes.

A total of 922 proteins were identified in the culture filtrate of strain OS7, many of them being cytoplasmic polypeptides, e.g. ribosomal proteins and histones. Thus, the proteomics method used was highly sensitive, and detected not only proteins actively exported into culture fluid, but also those released from lysed cells. Among the detected proteins, 59 were found only in the culture filtrate of strain OS7, but not in that of strain OS7mut1 (Table S2). An accurate estimation of protein abundance in a sample is generally difficult with MS analyses; however, a semi-quantitative method based on the protein abundance index (emPAI) is available¹⁶. In this method, the emPAI value is calculated by the equation: $10^{\text{PAI}-1}$, where PAI is the number of detected peptides divided by the theoretical number of peptides for each protein. Among these 59 proteins, the emPAI values were very low (emPAI < 1) for 56, and the 56 proteins might well be undetected in the filtrate of the OS7mut1 culture due to their low abundance. Thus, only three proteins were identified as being synthesized specifically in strain OS7 but not in strain OS7mut1. These three proteins were annotated as [NiFe] hydrogenase large and small subunits (*MMOS7_11590* and *MMOS7_11600*, respectively), and carbonic anhydrase (*MMOS7_11640*) (Table S2). These three were the products of the OS7/KA1-specific genes (Table S1).

Comparative genomics of strains OS7 and OS7mut1. We also carried out Illumina sequencing of the genomes of strains OS7 and OS7mut1 to identify mutations in strain OS7mut1 responsible for the Fe⁰-non-corroding phenotype. The genome size of strain OS7mut1 was 1,737,727 bp, which was 12,022 bp shorter than that of strain OS7. When the genome sequences of strains OS7 and OS7mut1 were aligned to the reference sequence of the OS7 genome as determined by classic Sanger sequencing, a 12,022-bp region spanning *MMOS7_11520* and *MMOS7_11650* was found to be deleted in the genome of strain OS7mut1 (Fig. 3(A)). As discussed below, this DNA segment seems to be a genomic island that can spread horizontally among methanogens. Because of this reason, we call this region the “MIC island”. In addition to MIC island deletion, the Illumina sequencing detected ambiguous bases at eight different sites in the genome of strain OS7mut1; at these sites, mixed bases were identified in different reads with an abundance greater than 10% for two or more bases. Since both the wild type and mutant sequences were mixed at these eight sites, we did not treat these sites as OS7mut1-specific mutations.

At both ends of the MIC island in the genomes of strain OS7 and KA1, nearly perfect 221 bp direct repeats were found; the 3'-end sequence of *MMOS7_11510*, which was almost identical (219/221) to the *MMOS7_11660* sequence (Fig. 3(B)). This observation implied that the deletion in strain OS7mut1 had occurred by homologous

recombination between the directly repeated sequences within *MMOS7_11510* and *MMOS7_11660* (Fig. S1), and that the deleted region in *OS7mut1* encoded function(s) necessary for MIC activity. This notion was further supported by PCR assays for the presence/absence of the MIC-island genes, *MMOS7_11550*, *MMOS7_11570*, *MMOS7_11590*, *MOS7_11600*, and *MMOS7_11630*. These genes were detected in corrosion-positive *M. maripaludis* strains KA1, OS7 and *Mic1c10*⁴, but not in corrosion-negative *M. maripaludis* strains, *OS7mut1*, S2, C5, C6, and C7.

[NiFe] hydrogenase as a causal agent of MIC. In the deleted region, 14 putative genes were identified, of which eight genes were functionally annotated. *MMOS7_11590* and *MMOS7_11600* were annotated to encode the small and large subunits, respectively, of a [NiFe] hydrogenase. Since hydrogenases catalyze the reversible oxidation of molecular hydrogen ($2\text{H}^+ + \text{A}_{\text{red}} \rightleftharpoons \text{H}_2 + \text{A}_{\text{ox}}$), we assume that this [NiFe] hydrogenase is capable of drawing electrons from Fe^0 , generating H_2 : $2\text{H}^+ + \text{Fe}^0 \rightleftharpoons \text{H}_2 + \text{Fe}^{2+}$; therefore, we hypothesized that this [NiFe] hydrogenase is the causal agent of MIC. We hereafter call this [NiFe] hydrogenase the “MIC hydrogenase”.

[NiFe] hydrogenases generally consist of large and small subunits¹⁷. Some [NiFe] hydrogenases contain a twin-arginine translocation (Tat) signal sequence (RRxFxK) on their small subunits, and are secreted through the cytoplasmic membrane by virtue of a Tat pathway^{18,19}. A Tat signal motif was found in the N-terminal region of the small subunit of the MIC hydrogenase indicating that the MIC hydrogenase was secreted across the cytoplasmic membrane. In archaea, the Tat pathway consists of TatA and TatC¹⁸. Interestingly, *MMOS7_11620* and *MMOS7_11630* were annotated to encode TatC and TatA, respectively. Thus, the *MMOS7_11620* and *MMOS7_11630* proteins were considered to form a Tat complex that recognizes the Tat secretion signal of the small subunit of the MIC hydrogenase, and the folded MIC hydrogenase (comprising the small and large subunit complexes of the MIC hydrogenase) was expected to be exported across the cytoplasmic membrane. Since the small and large subunits of the MIC hydrogenase were both detected in the culture filtrate of strain OS7 (Table S2), it is possible that the MIC hydrogenase exported across the cytoplasmic membrane is further excreted across the S-layer to the exterior of the cell.

To address this possibility, we carried out proteomics analysis of cells of strain OS7, and the emPAI values of cellular proteins per ml culture were compared with those of supernatant proteins per ml culture. Since the detection of proteins at emPAI levels below one was often not reproducible between two experiments (Table S2), 226 supernatant proteins with emPAI values higher than one were selected for the comparison. In Table S3, the emPAI values of cellular proteins collected from a 5.5-ml culture, emPAI(cell), and those of supernatant proteins collected from a 800-ml culture, emPAI(sup), are shown. These values were divided by the respective culture volumes, and the ratio, [emPAI(cells)/5.5]/[emPAI(sup)/800], was calculated for each of the 226 proteins. This ratio, relative protein abundance (cell/sup), would be less than one (with a certain degree of error) if more than half the amount of the protein is released into supernatant. The top 20 proteins showing the lowest ratio (in other words, the top 20 candidates for secreted proteins) were further examined (Table S3). The small and large subunits of the MIC hydrogenase (*MMOS7_11590* and *MMOS7_11600*) and carbonic anhydrase (*MMOS7_11640*) were included in the list. Among the listed proteins, the N-terminal signal sequence was predicted in 15 proteins. Among five proteins with no signal sequence, three were small in sizes: 61 aa for *MMOS7_12890* (30S ribosomal protein S27e), and 54 aa for *MMOS7_15050* and *MMOS7_15070*. The amino acid sequences of *MMOS7_15050* and *MMOS7_15070* were 100% identical, but their biological functions are unknown. These proteins were detected in the supernatant sample but not in the cell sample probably because those in the cell sample run off the bottom of a gel of SDS PAGE before they were subjected to MS/MS analysis. One of the two remaining proteins with no signal peptide was archaeal histone (*MMOS7_15990*) which is abundant in cells. Since the emPAI value for abundant proteins saturates¹⁶, it would be possible that the “relative protein abundance” value for archaeal histone shown in Table S3 was underestimated. The rest was the large subunit of [NiFe]-hydrogenase which is known to be exported by the Tat translocase as a heterodimer with the small subunit²⁰. Thus, the comparison between cytoplasmic proteome and secretome allowed the identification of secreted proteins with a high degree of confidence.

Genes required for the assembly of the MIC hydrogenase. The large subunit of [NiFe]-hydrogenases contains a NiFe(CN)₂CO metallo-center required for the activation of H₂, while the small subunit harbors three iron-sulfur clusters, namely a proximal [4Fe-4S] cluster, a mesial [3Fe-4S] cluster, and a distal [4Fe-4S] cluster^{21,22}. For the formation of NiFe(CN)₂CO metallo-center, six auxiliary Hyp (hydrogenase pleiotropic) proteins, namely, HypA, B, C, D, E and F, are necessary in addition to a chaperone protein, SlyD²³. The analogs of *hypA* (*MMKA1_03080*, *MMOS7_03350*), *hypB* (*MMKA1_17480*, *MMOS7_16300*), *hypC* (*MMKA1_15530*, *MMOS7_14340*), *hypD* (*MMKA1_02960*, *MMOS7_03230*), *hypE* (*MMKA1_02810*, *MMOS7_03080*), *hypF* (*MMKA1_01450*, *MMOS7_01710*) and *slyD* (*MMKA1_13650* or *MMKA1_06200*, *MMOS7_12980* or *MMOS7_06150*), were all found in the chromosomes of strains OS7 and KA1. After the insertion of the metallo-center, an endopeptidase removes the C-terminal extension of the large subunit. A gene for such an endopeptidase (*MMOS7_11610*) was found next to the structural genes for the MIC hydrogenase. In *Escherichia coli* expressing at least three [NiFe] hydrogenases, a single set of HypA-HypF proteins are involved in the insertion of the metallo-center in the three hydrogenases. However, for the cleavage of their C-terminal extension, each hydrogenase requires its own specific endopeptidase encoded within the same operon¹⁷. This rule could also be applied to the MIC hydrogenase.

MIC hydrogenase is a novel family member of [NiFe] hydrogenases. To date, [NiFe] hydrogenases have been classified into four groups based on their amino acid sequences, the organization of their genes, and their biochemical characteristics^{17,24}. Phylogenetic analysis of the large and small subunits of the MIC

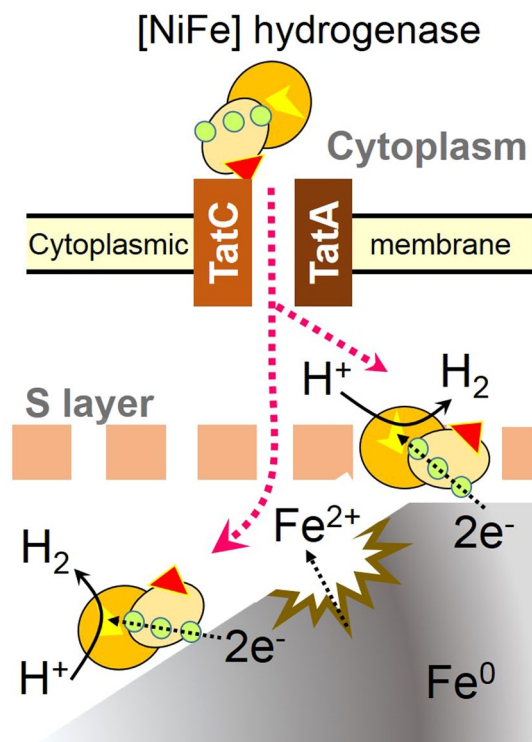


Figure 4. Model of Fe^0 corrosion enhanced by MIC hydrogenase. Two spheres of a [NiFe] hydrogenase represent the large and small subunits. A yellow patch on the large subunit represents the catalytic center that catalyzes reversible oxidation of H_2 . Three circles on the small subunit represent proximal, mesial, and distal iron-sulfur clusters that transfer electrons from an electron donor to the catalytic center to form H_2 . A red triangle on the small subunit represents a Tat signal peptide that is recognized by TatC. TatA and TatC constitute the TatA/TatC translocator through which the MIC hydrogenase is secreted through the cytoplasmic membrane. After completion of the translocation, the signal peptide is removed by a signal peptidase. The MIC hydrogenase localizes either on the surface of, or outside, the S-layer to receive electrons from Fe^0 .

hydrogenase revealed that these proteins were located outside the four known groups of [NiFe] hydrogenases indicating that the MIC hydrogenase is a novel type of [NiFe] hydrogenase (Fig. S2).

The alignment of the small subunit of the MIC hydrogenase with published small subunit sequences revealed that the residues coordinating the proximal [4Fe-4S], mesial [3Fe-4S], or distal [4Fe-4S] cluster were well conserved in the small subunit of the MIC hydrogenase (Fig. S3). In the active form of the $\text{NiFe}(\text{CN})_2\text{CO}$ metallo-center in the large subunit of [NiFe] hydrogenases, the nickel atom is coordinated either with two cysteines or with one selenocysteine and one cysteine, while the iron atom is bridged to the nickel atom by two cysteinyl sulfur ligands^{20,21}. These amino acids were conserved, while no selenocysteine was found in the large subunit of the MIC hydrogenase (Fig. S4).

Model of hydrogenase-induced Fe^0 corrosion. Our model of the MIC-hydrogenase-induced Fe^0 corrosion, which is similar to those proposed previously^{5,13} is depicted in Fig. 4. We postulate that the MIC hydrogenase directly contacts the Fe^0 surface, where the hydrogenase receives electrons from Fe^0 to form H_2 using H^+ from water. To be able to do so, the MIC hydrogenase should either be excreted outside the cell or be presented at the external surface of the S-layer. As already discussed above, the MIC hydrogenase was predicted to be secreted in a Tat-dependent manner. Furthermore, we showed that the enzyme was excreted in culture medium (Fig. 2 and Table S3). However, it is still unclear whether the excretion of the MIC hydrogenase occurs either through the intact S layer or through damaged S-layer structure.

For proton reduction by [NiFe] hydrogenases, electrons are transferred from a redox partner, such as NADH, reduced ferredoxin or reduced cytochrome c_3 , to the Ni-Fe active site via three (distal, mesial and proximal) iron-sulfur clusters^{21,22}. The distal iron-sulfur cluster is exposed to the molecular surface, and can directly interact with a specific redox partner. Thus, it is interesting to resolve the 3D structure of the MIC hydrogenase to understand how this enzyme contacts the Fe^0 surface. In addition, the determination of redox potentials of the three iron-sulfur clusters of the MIC hydrogenase would be important, as these iron-sulfur clusters should have appropriate redox potentials for the efficient delivery of electrons from Fe^0 to H^+ via the catalytic center of the MIC hydrogenase²⁵.

Several studies have reported that hydrogenases from different microorganisms stimulated the oxidation of Fe^0 with concomitant hydrogen evolution^{5,26}. In addition, other redox enzymes such as formate dehydrogenase¹³ and heterodisulfide reductase supercomplex²⁷ also stimulate the Fe^0 oxidation. From these observations, certain redox enzymes seemed to be able to oxidize Fe^0 when they come into contact with the Fe^0 surface. However, redox enzymes which do not possess Tat or Sec-dependent signal sequences cannot interact with external Fe^0 . Thus, one

of the reasons why most hydrogenase-bearing microorganisms are not Fe⁰-corrosive in laboratory conditions may be because they do not express extracellular redox enzymes. It should however be noted that microorganisms that do not secrete extracellular redox enzymes could also be involved in MIC in natural environments, e.g. in biofilms developed on metal substrata, through release of redox enzymes from lysed cells¹³.

Possible roles of γ -carbonic anhydrase in MIC. A gene encoding γ -carbonic anhydrase (MMOS7_11640) bearing a *sec*-dependent signal peptide at its N-terminal region was identified within the MIC island, suggesting that this enzyme was secreted across the cytoplasmic membrane. This inference was confirmed by proteomics analyses (Tables S2 and S3). Carbonic anhydrases catalyze the reversible hydration of CO₂ to bicarbonate: CO₂ + H₂O \rightleftharpoons HCO₃⁻ + H⁺. Since CO₂ is an indispensable electron acceptor in methanogens, carbonic anhydrase in the cytoplasm may be important to convert bicarbonate to CO₂, which is then used in the first committed step of methanogenesis. On the other hand, the role of extracellular carbonic anhydrases is not clear, one possibility being the conversion of CO₂ to bicarbonate, which can be transported within cells by a bicarbonate transporter²⁸.

In the presence of Fe²⁺ and bicarbonate, ferrous carbonate is formed: Fe²⁺ + HCO₃⁻ = FeCO₃ + H⁺. Under such conditions, the external carbonic anhydrase could contribute indirectly to the formation of FeCO₃ by converting CO₂ into bicarbonate. However, more studies are needed to elucidate the roles of the extracellular carbonic anhydrase in the Fe⁰ corrosion and the proliferation of methanogens containing the MIC island.

Genetically unstable MIC island. We concluded that the MIC island is unstable in the genomes of strains OS7 and KA1 from the following two observations. First, in an early stage of the KA1 genome sequencing study using the Sanger method, we found two different genes downstream of the *MMOS7_11510* ortholog. In some shotgun clones, the downstream gene was an *MMOS_11520* ortholog, as seen in the genome of strain OS7, while the *MMOS_11670* ortholog was the downstream gene in other shotgun clones as seen in the genome of strain OS7mut1 (Fig. 3). We interpreted this observation as indicating that a culture of strain KA1 from which DNA was prepared for the genome sequencing study was heterogeneous, and contained wild-type cells and spontaneous deletion mutants lacking the MIC-island. Second, cultures of strain OS7 grown under H₂ + CO₂ often showed very low MIC activities suggesting that a significant proportion of the cell population in culture lost the MIC island. In fact, strain OS7mut1 was isolated from one of such cultures.

We thus inferred that the MIC island could readily be excised through homologous recombination at the direct repeat sequences, excising a circular DNA and leaving a hybrid gene of *MMOS7_11510* and *MMOS7_11660* in the chromosome (Fig. S1(A)). The function of *MMOS7_11510* is not clear. It encodes a protein belonging to the family of “putative methanogenesis marker protein 1” according to the INTERPRO classification (IPR017667), which is widely distributed in methanogens.

Once the excised circular DNA is transferred into other hosts through conjugation, transduction, or transformation, the MIC island can be integrated into the chromosome of the new host at the *MMOS7_11510*-ortholog site via homologous recombination (Fig. S1(B)). Thus, the genetic instability of the MIC island provides a means of horizontal transfer of the MIC island among methanogens.

As described in the Introduction section, the Fe⁰-corroding activities in two strains of *M. maripaludis*, MM901 and MM1284, were investigated by Deutzmann *et al.*¹³. Strain MM901 was isolated from strain S2 by disrupting the uracil phosphoribosyltransferase gene, while strain MM1284 was isolated from strain MM901 by disrupting five hydrogenase genes (*vhuU*, *vhcA*, *fruA*, *frcA*, *hmd*, and *ehbN*) and one dehydrogenase gene (*hmd*). Strain MM901 showed enhanced Fe⁰-corroding activity, whereas strain MM1284 did not. These results are inconsistent to ours. As shown in Fig. 1, strain S2, which is the parental strain of MM901, did not exhibit Fe⁰-corroding activity. Strain S2 carries genes for the subunits of six [NiFe] hydrogenases, namely the subunit genes for two coenzyme F₄₂₀-reducing hydrogenases (*Mmp1382* - 1385; and *Mmp0817* - 0820), those for two non-F₄₂₀-reducing hydrogenases (*vhu*: *Mmp1692* - 1696; and *vhc*: *Mmp0821* - 0824) and those for two energy-conserving hydrogenases (*eha*: *Mmp1448* - 1467; and *ehb*: *Mmp0400*, 0940, 1049, 1073, 1074, 1153, 1469, and 1621-1629). This strain also carries two H₂-dependent methylene tetrahydromethanopterin dehydrogenase genes (*hmd*: *Mmp0127*; and *hmd* paralog: *Mmp1716*)²⁹. Strains KA1, OS7, and OS7mut1 carry orthologs of all the genes. Nevertheless, strain OS7mut1 was deficient in Fe⁰-corroding activity.

We attributed these contradictory results to the instability of the MIC island. We hypothesize that strain S2 originally possessed the MIC island, as did strain MM901, but the MIC island in strain S2 was lost before we acquired it. Similarly, the MIC island in strain MM1284 was lost before Deutzmann *et al.*¹³ performed their experiments. Strain S2 has been usually maintained and distributed with H₂ as a sole electron donor. This cultivation condition does not prevent the loss of Fe⁰-corrosion ability as described before. To avoid the accumulation of MIC-island-free derivatives, we often purify colonies of strains OS7 and KA1 by the agar shake tube technique, and MIC-positive clones were preserved in basal medium supplemented with 20% glycerol at -80 °C. This precaution is very important for researchers studying MIC-inducing methanogens, and possibly MIC-inducing SRBs.

Evolution of the MIC island. Recently, the genome sequence of *Methanobacterium congolense* strain Buetzberg was published³⁰. Homology at the nucleotide sequence level was not high between the genome sequence of strain OS7 and that of strain Buetzberg, with the exceptions of several limited regions. One such region showed extensive homology to the MIC island (Fig. 5) indicating that gene clusters related to the MIC island have spread among methanogens beyond the genus level.

Careful comparison of the nucleotide sequences of the MIC islands in strains OS7/KA1 and strain Buetzberg gave an insight into how the MIC island in strain OS7/KA1 has evolved. As shown in Fig. 5, the first gene of the MIC island, *MMOS7_11520*, was homologous to *MCBB_1249*, while the last gene of the MIC island, *MMOS7_11650*, was homologous to the 5'-half of *MCBB_1258* (Figs 5 and S5). *MCBB_1258* encoded two types of

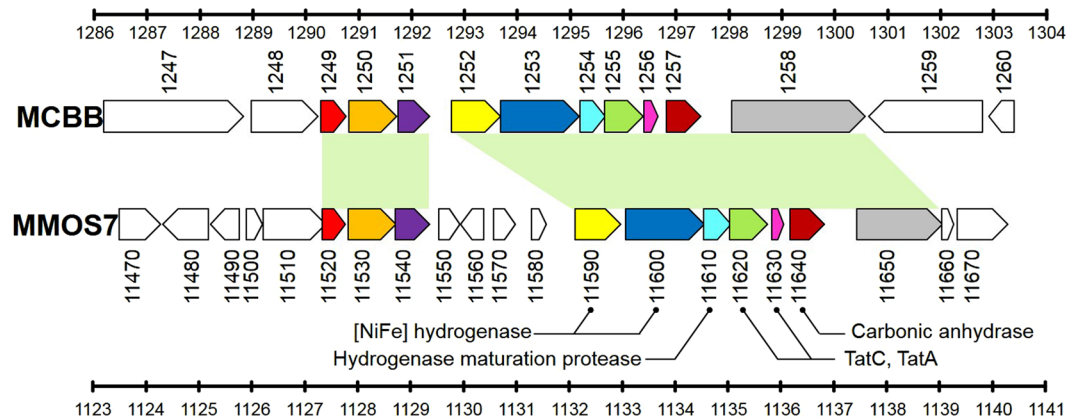


Figure 5. Genome map of strain Buetzberg at coordinates 1,286 to 1,304 kb and that of strain OS7 at 1,123 to 1,141 kb. The upper part shows genes of strain Buetzberg (*MCBB_1247* to *MCBB_1260*), while the lower part shows genes of strain OS7. Both regions contained homologous genes that are shown in the same colors.

domains, PAS and GAF; both are found in many proteins involved in signal transduction, while *MMOS7_11650* only encoded the PAS domain. Thus, we considered *MCBB_1258* as representing the conserved ancestral gene structure, while *MMOS7_11650* is a truncated derivative of the ancestral gene. Four genes, *MMOS7_11550*, *MMOS7_11560*, *MMOS7_11570*, and *MMOS7_11580*, found in the MIC island of strain OS7, were absent in the island of strain Buetzberg. These four genes might have been either acquired in the island of strain OS7 by horizontal gene transfer, or deleted from an ancestral island in strain Buetzberg.

The 74 bp-long 3'-end sequence of *MMOS7_11510* overlaps with the 5'-end of *MMOS7_11520*, which is the first gene of the MIC island in strain OS7 [Fig. S5(A), underlined sequence]. As mentioned previously, the 3'-end sequence of *MMOS7_11510* was almost identical to the *MMOS7_11660* sequence except for the last nine nucleotides: [AAAAATTGA; Fig. 3(B)]. This AAAAATTGA sequence was rather similar to the aligned *MCBB_1249* sequence [Figure S5(A), green underlined sequence]. This observation suggested that the 3'-end sequence of an ancestral *MMOS7_11510* locus was TTAAATTTAATTTAA found in *MMOS7_11660* [Figs 3(B) and S5(B)], and that the 5'-end of the current MIC island in strain OS7 (the *MMOS7_11520*) had been formed by the fusion between the ancestral *MMOS7_11510* with the deletion at the 3'-end (TTAAATTTAATTTAA) and an ancestral *MCBB_1249* (the first gene of an ancestral MIC island) with a deletion of more than 100 bp at the 5'-end (Fig. S5(B)).

The 3'-end sequence of *MMOS7_11650* (ATGCCAAATAA: bold and underlined sequence in Fig. S6) which corresponds to the 3'-end region of the MIC island in strain OS7 overlaps with the 5'-end of *MMOS7_11660*. Since the ATGCCAAATAA sequence was also found in *MMOS7_11510* [Fig. 3(B), green sequence], we inferred that the ATGCCAAATAA sequence existed in the ancestral *MMOS7_11510*. On the other hand, *MCBB_1258* has the ATGCCAAA(GAT) sequence at the corresponding site (Fig. S6, red sequence). Hence, the 3'-end of the current MIC island in strain OS7 (the *MMOS7_11650*-*11660* junction) would be formed by the fusion of the ancestral *MCBB_1258* and the ancestral *MMOS7_11510* by homologous recombination at the ATGCCAAA sequence. These inferences are summarized in Fig. S7.

In the MIC island, the genes for the small and large subunits of the MIC hydrogenase, a TatA/TatC translocase, and a hydrogenase maturation protease are encoded. The clustering of the genes required for the functional expression of the MIC hydrogenase in a single genomic island may provide evolutionary advantages as the maturation of a [NiFe] hydrogenase requires a specific hydrogenase maturation protease³¹, and the Tat export system is not common in methanogens¹⁹. The presence of the MIC hydrogenase thus may increase the fitness of methanogens thriving in environments with access to steel structures, where Fe⁰ is available as a source of electrons.

Horizontal gene transfer plays an important role in the evolution of microorganisms, where genomic islands encoding various functions contribute to rapid propagation of specific traits among prokaryotes in local environments³². As discussed above, the MIC island can be transferred into other hosts through a homologous recombination-mediated mechanism (Fig. S1). However, the MIC island seems to encode no enzyme involved in transposition. Therefore, horizontal transfer events of the MIC island may occur at a very low frequency. On the other hand, methanogens possessing the MIC island, once acquired, would be enriched in environments where Fe⁰ is available as a source of electron, and increase the risk of MIC with time. Since the increasing occurrence of methanogens possessing the MIC island is a global industrial concern, the presence, persistence, and potential transfer of the MIC island among populations should be investigated in model environments such as pipelines, in parallel to the development of methods to control MIC-causing methanogens. Our findings provide a basis for the development of molecular tools to monitor epidemiology, and to perform surveillance and risk assessment of MIC-inducing *M. maripaludis*.

Materials and Methods

Strains, media, and culture conditions. *M. maripaludis* strains, KA1¹¹ (=NBRC 102054), S2^{29,33} (=NBRC 101832), C5³³ (=NBRC 102114), C6³³ (=JCM 10012), and C7³³ (=JCM 10012) were obtained from NITE Biological Resource Center (<https://www.nite.go.jp/en/nbrc/index.html>) and Japan Collection of Microorganisms (<http://jcm.brc.riken.jp/en/>), while *M. maripaludis* strains OS7 (=NBRC 103642) and OS7mut1 (=NBRC 105638) were isolated in this study.

Basal medium, which is “Artificial seawater medium”³⁴ supplemented with 100 mM sodium 2-[4-(2-Hydroxyethyl)-1-piperazinyl] ethanesulfonate (pH 7.0) and 0.1% (w/v) L-cysteine hydrochloride monohydrate, was used to cultivate *M. maripaludis* strains with two different methods. In the first method, where H₂ was an electron donor and CO₂ was an electron acceptor, cells were cultivated at 37 °C in a 70 ml serum bottle containing 20 ml basal medium under a H₂ + CO₂ gas mixture (80:20, 1.78 atm). In the second method, where Fe⁰ was an electron donor and CO₂ was an electron acceptor, cells were cultivated at 37 °C in a 70 ml serum bottle containing 20 ml basal medium and 6 g of Fe⁰ granules (1 to 2 mm in diameter and 99.98% purity) under the N₂ + CO₂ gas mixture (80:20, 1 atm). The bottles were sealed with butyl rubber stoppers.

Determination of Fe⁰-corroding activities of *M. maripaludis* strains and their culture filtrates.

One milliliter of a preculture of strain OS7, OS7mut1, S2, C5, C6, or C7 grown in 20 ml of basal medium under H₂ + CO₂ at 37 °C for 10 days was transferred into 20 ml basal medium containing Fe⁰ granules, and cultivated under N₂ + CO₂ at 37 °C for 14 days. A sterile control was also incubated under the same conditions. The concentrations of Fe²⁺, CH₄, and H₂ generated from the cultures were determined as described previously¹¹. All assays were conducted using four replicates.

A culture of strain OS7 grown at 37 °C for 10 days in 20 ml basal medium under H₂ + CO₂ was filtered through a 0.22 μm filter, and 1 ml of the filtrate was added to 20 ml basal medium containing Fe⁰ granules under N₂ + CO₂. The medium containing the filtrate was either untreated (OS7 filtrate), or treated either with 100 μl of proteinase K (Qiagen; >600 mAU/ml; one mAU releases 1 μmol tyrosine per min from hemoglobin at 37 °C, pH7.5) at 50 °C for 20 min followed by the heat treatment at 100 °C for 5 min (OS7 filtrate + K), or without Qiagen proteinase K at 50 °C for 20 min (OS7 filtrate +50 °C). As a sterile control, 21 ml basal medium containing Fe⁰ granules was treated with 100 μl Qiagen proteinase K under N₂ + CO₂ at 50 °C for 20 min followed by the treatment at 100 °C for 5 min (Control + K). The duplicated samples thus prepared were incubated at 37 °C for 14 days under N₂ + CO₂, and the concentrations of Fe²⁺, CH₄, and H₂ in the samples were determined as described above.

Omics studies. The methods employed for genome and proteome analyses are described in the Supplementary Materials and Methods.

Data Availability

Complete genome sequences of *M. maripaludis* strains OS7, OS7mut1, and KA1 were deposited in DDBJ/EMBL/GenBank under the accession numbers AP011528, CP020120, and AP011526, respectively. Other datasets generated during and/or analyzed during the current study are available from the corresponding author on reasonable request.

References

- Enning, D. & Garrelfs, J. Corrosion of iron by sulfate-reducing bacteria: New views of an old problem. *Appl. Environ. Microbiol.* **80**, 1226–1236 (2014).
- Enning, D. *et al.* Marine sulfate-reducing bacteria cause serious corrosion of iron under electroconductive biogenic mineral crust. *Environ. Microbiol.* **14**, 1772–1787 (2012).
- Dinh, H. T. *et al.* Iron corrosion by novel anaerobic microorganisms. *Nature* **427**, 829–832 (2004).
- Mori, K., Tsurumaru, H. & Harayama, S. Iron corrosion activity of anaerobic hydrogen-consuming microorganisms isolated from oil facilities. *J. Biosci. Bioeng.* **110**, 426–430 (2010).
- Zadvorny, O. A., Zorin, N. A. & Gogotov, I. N. Transformation of metals and metal ions by hydrogenases from phototrophic bacteria. *Arch. Microbiol.* **184**, 279–285 (2006).
- Venzlaff, H. *et al.* Accelerated cathodic reaction in microbial corrosion of iron due to direct electron uptake by sulfate-reducing bacteria. *Corros. Sci.* **66**, 88–96 (2013).
- Beese-Vasbender, P. F., Nayak, S., Erbe, A., Stratmann, M. & Mayrhofer, K. J. J. Electrochemical characterization of direct electron uptake in electrical microbially influenced corrosion of iron by the lithoautotrophic SRB *Desulfopila corrodens* strain IS4. *Electrochim. Acta* **167**, 321–329 (2015).
- Pirbadian, S. *et al.* *Shewanella oneidensis* MR-1 nanowires are outer membrane and periplasmic extensions of the extracellular electron transport components. *Proc. Natl. Acad. Sci.* **111**, 12883–12888 (2014).
- Deng, X., Nakamura, R., Hashimoto, K. & Okamoto, A. Electron extraction from an extracellular electrode by *Desulfovibrio ferrophilus* strain IS5 without using hydrogen as an electron carrier. *Electrochemistry* **83**, 529–531 (2015).
- Daniels, L., Belay, N., Rajagopal, B. S. & Weimer, P. J. Bacterial methanogenesis and growth from CO₂ with elemental iron as the sole source of electrons. *Science* **237**, 509–511 (1987).
- Uchiyama, T., Ito, K., Mori, K., Tsurumaru, H. & Harayama, S. Iron-corroding methanogen isolated from a crude-oil storage tank. *Appl. Environ. Microbiol.* **76**, 1783–1788 (2010).
- Kip, N. *et al.* Methanogens predominate in natural corrosion protective layers on metal sheet piles. *Scientific reports* **7**, 11899 (2017).
- Deutzmann, J. S., Sahin, M. & Spormann, A. M. Extracellular enzymes facilitate electron uptake in biocorrosion and bioelectrosynthesis. *mBio* **6**, e00496–15 (2015).
- Hungate, R. E. *A roll tube method for cultivation of strict anaerobes in Methods in Microbiology*, vol. 3B. (eds Norris, J. R. & Ribbons, D. W.) 117–132 (Academic Press, 1969).
- Jones, W. J., Whitman, W. B., Fields, R. D. & Wolfe, R. S. Growth and plating efficiency of methanococci on agar media. *Appl. Environ. Microbiol.* **46**, 220–226 (1983).
- Ishihama, Y. *et al.* Exponentially modified protein abundance index (emPAI) for estimation of absolute protein amount in proteomics by the number of sequenced peptides per protein. *Mol. Cell. Proteomics* **4**, 1265–1272 (2005).
- Vignais, P. M. & Billoud, B. Occurrence, classification, and biological function of hydrogenases: An overview. *Chem. Rev.* **107**, 4206–4272 (2007).

18. Wu, L. F., Chanal, A. & Rodrigue, A. Membrane targeting and translocation of bacterial hydrogenases. *Arch. Microbiol.* **173**, 319–324 (2000).
19. Dilks, K., Rose, R. W., Hartmann, E. & Pohlschroder, M. Prokaryotic utilization of the twin-arginine translocation pathway: A genomic survey. *J. Bacteriol.* **185**, 1478–1483 (2003).
20. Thauer, R. K. *et al.* Hydrogenases from methanogenic archaea, nickel, a novel cofactor, and H₂ storage. *Ann. Rev. Biochem.* **79**, 507–536 (2010).
21. Ogata, H., Lubitz, W. & Higuchi, Y. Structure and function of [NiFe] hydrogenases. *J. Biochem.* **160**, 251–258 (2016).
22. Garcin, E. *et al.* The crystal structure of a reduced [NiFeSe] hydrogenase provides an image of the activated catalytic center. *Structure* **7**, 557–566 (1999).
23. Peters, J. W. *et al.* [FeFe]- and [NiFe]-hydrogenase diversity, mechanism, and maturation. *Biochim. Biophys. Acta Molecular Cell Research* **1853**, 1350–1369 (2015).
24. Greening, C. *et al.* Genomic and metagenomic surveys of hydrogenase distribution indicate H₂ is a widely utilized energy source for microbial growth and survival. *ISME J.* **10**, 761–777 (2015).
25. Adamson, H. *et al.* Retuning the catalytic bias and overpotential of a [NiFe]-hydrogenase via a single amino acid exchange at the electron entry/exit site. *J. Am. Chem. Soc.* **139**, 10677–10686 (2017).
26. Mehanna, M. *et al.* New hypotheses for hydrogenase implication in the corrosion of mild steel. *Electrochim. Acta* **54**, 140–147 (2008).
27. Lienemann, M., Deutzmann, J. S., Milton, R. D., Sahin, M. & Spormann, A. M. Mediator-free enzymatic electrosynthesis of formate by the *Methanococcus maripaludis* heterodisulfide reductase supercomplex. *Bioresour. Technol.* **254**, 278–283 (2018).
28. Smith, K. S. & Ferry, J. G. Prokaryotic carbonic anhydrases. *FEMS Microbiol. Rev.* **24**, 335–366 (2000).
29. Hendrickson, E. L. *et al.* Complete genome sequence of the genetically tractable hydrogenotrophic methanogen *Methanococcus maripaludis*. *J. Bacteriol.* **186**, 6956–6969 (2004).
30. Tejerizo, G. T. *et al.* Genome sequence of *Methanobacterium congolense* strain Buetzberg, a hydrogenotrophic, methanogenic archaeon, isolated from a mesophilic industrial-scale biogas plant utilizing bio-waste. *J. Biotech.* **247**, 1–5 (2017).
31. Lacasse, M. J. & Zamble, D. B. [NiFe]-hydrogenase maturation. *Biochemistry* **55**, 1689–1701 (2016).
32. Cordero, O. X. & Polz, M. F. Explaining microbial genomic diversity in light of evolutionary ecology. *Nat. Rev. Microbiol.* **12**, 263–273 (2014).
33. Whitman, W. B., Shieh, J., Sohn, S., Caras, D. S. & Premachandran, U. Isolation and characterization of 22 mesophilic methanococci. *Syst. Appl. Microbiol.* **7**, 235–240 (1986).
34. Widdel, F. & Bak, F. *Gram-negative mesophilic sulfate-reducing bacteria in The Prokaryotes* (eds Balows, A., Trüper, H. G., Dworkin, M., Harder, W. & Schleifer, K. H.) 3352–3378 (Springer, 1992).

Acknowledgements

We thank Seishi Ikeda (National Agriculture and Food Research Organization) and Kimio Ito (Nippon Steel and Sumitomo Metal Corporation) for helpful discussions. We also thank Ayako Koide (NITE) for technical assistance. The study was partially supported by the New Energy and Industrial Technology Development Organization (NEDO) (grant no. P05032).

Author Contributions

H.T., K.M., T.U. and T.I. contributed to the isolation of strains OS7 and performed corrosion assays. H.T., H.A., K.N., M.M., J.Y., K.S. and S.Y. contributed to the isolation of OS7mut1. H.T. and S.H. wrote the manuscript. Nao.I., K.M., A.H., A.S., T.H., H.H., T.S., K.J. and S.T. sequenced the genomes of strains OS7, KA1 and OS7mut1. Nao.I., Nat.I., T.S. and S.T. performed the genome annotation of strains OS7 and KA1. S.W. performed a PCR survey for the MIC island genes in *M. maripaludis* strains. H.A., K.N., M.M., J.Y., K.S. and S.Y. performed proteomic analysis. N.F. designed and supervised the genome and proteome analyses. S.H. conceived, designed, and supervised the project. All co-authors have read the manuscript and agreed to the final version for publication.

Additional Information

Supplementary information accompanies this paper at <https://doi.org/10.1038/s41598-018-33541-5>.

Competing Interests: The authors declare no competing interests.

Publisher's note: Springer Nature remains neutral with regard to jurisdictional claims in published maps and institutional affiliations.



Open Access This article is licensed under a Creative Commons Attribution 4.0 International License, which permits use, sharing, adaptation, distribution and reproduction in any medium or format, as long as you give appropriate credit to the original author(s) and the source, provide a link to the Creative Commons license, and indicate if changes were made. The images or other third party material in this article are included in the article's Creative Commons license, unless indicated otherwise in a credit line to the material. If material is not included in the article's Creative Commons license and your intended use is not permitted by statutory regulation or exceeds the permitted use, you will need to obtain permission directly from the copyright holder. To view a copy of this license, visit <http://creativecommons.org/licenses/by/4.0/>.

© The Author(s) 2018